A DISSERTATION
FOR THE DEGREE OF MASTER

Optical Coherence Tomography of the Tokay Gecko (*Gekko gecko*) eye

광간섭 단층촬영을 이용한 게코 도마뱀 눈의 형태 측정

by
Seokmin Go

MAJOR IN VETERINARY CLINICAL SCIENCES
DEPARTMENT OF VETERINARY MEDICINE
GRADUATE SCHOOL
SEOUL NATIONAL UNIVERSITY

February, 2020

Optical Coherence Tomography of the Tokay Gecko (*Gekko gecko*) eye

by

Seokmin Go

Supervised by
Professor Kangmoon Seo

Thesis
Submitted to the Faculty of the Graduate School
of Seoul National University
in partial fulfillment of the requirements
for the Degree of Master
in Veterinary Medicine

October, 2019

Major in Veterinary Clinical Sciences
Department of Veterinary Medicine
Graduate School
Seoul National University

December, 2019

Optical Coherence Tomography of the Tokay Gecko (*Gekko gecko*) eye

광간섭 단층촬영을 이용한 게코 도마뱀 눈의 형태 측정

지도교수 서 강 문

이 논문을 수의학 석사 학위논문으로 제출함
2019 년 10 월

서울대학교 대학원
수의학과 임상수의학 전공
고 석 민

고석민의 석사학위논문을 인준함
2019 년 12 월

위 원 장 _____ (인)

부위원장 _____ (인)

위 원 _____ (인)

Optical Coherence Tomography of the Tokay Gecko (*Gekko gecko*) eye

Supervised by

Professor Kangmoon Seo

Seokmin Go

Major in Veterinary Clinical Sciences,

Department of Veterinary Medicine Graduate School,

Seoul National University

ABSTRACT

This study was conducted to provide images of anterior and posterior structures of the gecko eye using spectral-domain optical coherence tomography (SD-OCT). Eight ophthalmologically normal Tokay geckos (*Gekko gecko*) participated. Nose-cloaca distance and body weight were measured for each gecko. Tomographic images were obtained using SD-OCT without anesthetic or mydriatic agents. The central corneal thickness (CCT), the anterior chamber depth (ACD), and the length of the conus papillaris (CP) were manually measured using OCT images. The thickness of the retinal nerve fiber layer (RNFL) around the CP, and the retinal thickness in quadrants (superior, nasal, inferior, and temporal area) were

automatically measured with OCT images. The mean values of the nose-cloaca distance and body weight were 13.8 ± 0.9 cm and 41.3 ± 9.0 g, respectively. The mean values of CCT, ACD, and CP length were 177.6 ± 20.9 μm, 1205.0 ± 79.9 μm, and 1546.4 ± 208.8 μm, respectively. The mean value of RNFL thickness was 52.0 ± 8.2 μm, and the thickest region was the superior region. The mean value of total retinal thickness was 202.5 ± 9.4 μm, and the thickest region was the temporal region. In conclusion, tomographic images of the anterior and posterior segments of the living gecko eye were obtainable using the OCT unit. Multiple retinal layers and anatomical features of the CP were identified.

Key words: conus papillaris, cornea, optical coherence tomography, retina, Tokay gecko

Student number: 2018-26091

CONTENTS

INTRODUCTION

Optical coherence tomography (OCT) is a high-resolution imaging technique that uses low-coherence light to obtain cross-sections of ocular tissue layers (Smith *et al*., 2013). In humans with retinal disorders, the use of OCT is not unfamiliar and many studies evaluating the optic nerve head, retinal nerve fiber layer, and macula have been done (Leung *et al*., 2010). Veterinary use of OCT has been reported frequently in mammals such as dogs and cats (Graham *et al*., 2019; Bemis *et al*., 2017; Hernandez-Merino *et al*., 2011; Gekeler *et al*., 2007; Espinheira Gomes *et al*., 2019; Rodarte-Almeida *et al*., 2016; Somma *et al*., 2017; Osinchuck *et al*., 2019). The relationship between retinal structure abnormalities and vision-related diseases including retinal dysplasia (Rodarte-Almeida *et al*., 2016), progressive retinal atrophy (Somma *et al*., 2017), sudden acquired retinal degeneration syndrome (SARDS) (Osinchuck *et al*., 2019), and glaucoma (Graham *et al*., 2019) has been studied in dogs. There are a few studies on reptilian species (saurians, ophidians, and chelonians) (Rival *et al*., 2015; Cazalot *et al*., 2015). However, to the authors' knowledge, those studies only took images of the cornea and anterior chamber, and there are no published studies of OCT parameters in the posterior segment of eyes in reptiles.

The retinal structures of lizards differ significantly when compared to mammals. Their retinas are avascular and nourished by a vascular conus papillaris (CP) that extends into the vitreous from the optic nerve (Girling and Raiti, 2004; Wyneken, 2012). Furthermore, the nocturnal Tokay gecko (*Gekko gecko*) and the diurnal American chameleon (*Anolis carolinensis*) have retinas formed of only rods and only

cones, respectively (Yokoyama and Blow, 2001). The ratio of rods to cones is known to be related to animal behavior, where diurnal animals have a higher proportion of cones and nocturnal animals have a higher proportion of rods (Wyneken, 2012). Most nocturnal lizards do not have fovea, but most diurnal lizards have one or two fovea (Wyneken, 2012; Sannan *et al*., 2018). These characteristics have made them good subjects for studying adaptations of the visual system to different environments (Yovanovich *et al*., 2019). Geckos have been used as experimental models in comparative biology, embryology and behavioral ecology (Higham and Schmitz, 2019; Fleishman *et al*., 2017; Putman *et al*., 2017). In order to fully characterize the gecko as an experimental model, it is important to obtain anatomical knowledge and quantitative data about the gecko eye.

High-quality imaging techniques are essential for understanding the anatomy of tissues. Optical coherence tomography can be used to obtain detailed images non-invasively from the eye. The purpose of this study was to observe the structure of gecko eyes using SD-OCT and to determine if OCT could be used as a diagnostic tool in small and exotic animals.

MATERIALS AND METHODS

1. Animals examined

Eight privately owned Tokay geckos (16 eyes) were used in this study. Prior to the OCT scanning, ophthalmic examinations including slit lamp biomicroscopy (SL-D7; Topcon, Japan) and rebound tonometry (Icare® Tonovet, Icare, Finland; "d" mode) were performed on all geckos to rule out any ocular diseases. No sedatives or anesthetic agents were used to avoid risks associated with anesthesia. Nose-cloaca distance and body weight were measured as parameters representing the size of animals. For obtaining histological structure of gecko retinas, formalin-fixed eyes from one gecko were submitted to a research and analysis company (GENOSS Co., Suwon, Korea). The globes were stained with hematoxylin and eosin. All experimental procedures were conducted according to the guidelines of and with the approval of the Institutional Animal Care and Use Committee (IACUC) of Seoul National University (SNU-190830-3).

2. OCT scanning

All images were obtained using SD-OCT (Optovue iVue, Inc; Freemont, CA) under dark-adapted conditions. An error occurred if the pupil size was smaller than the reference value of the OCT machine. As a result, we waited until the pupil size increased voluntarily larger than the size where no error would occur. Each animal was carefully handled during all experiments to minimize stress. Each gecko was manually restrained in one hand by supporting the jaw and forehead with index finger and thumb, while the body was supported in the palm. All experiments proceeded to the right eye (OD) first and then to the left eye (OS). All parameter measurements and OCT imaging of gecko eyes were performed by one examiner (SG).

3. Central corneal thickness and anterior chamber depth

The pupil was positioned in the center of the camera screen, and images were taken when the cornea was in focus. Two parameters were evaluated for each eye: (i) central corneal thickness (CCT), and (ii) anterior chamber depth (ACD). The CCT was defined as the distance between the corneal epithelium and endothelium in the region of the corneal apex. The ACD was defined as the distance between the corneal endothelium in the corneal apex and the anterior pole of the lens capsule.

4. Retinal nerve fiber layer thickness, conus papillaris length, and retinal thickness

By moving the focusing camera, the pupil was positioned in the center of the guide screen, and the CP was located in the center of the pupil. Then, the camera was moved forward or back until the retina was found in the OCT image. A series of posterior segment scans programmed on the OCT device were applied to all 16 eyes as follows: (i) optic nerve head (ONH) scan, (ii) retina cross-section scan, (iii) retina map scan, and (iv) three-dimensional (3D) view.

The ONH scan measured the thickness of the peripapillary retinal nerve fiber layer (RNFL) made up of ganglion cell axons. RNFL thickness was evaluated by quadrant (superior, nasal, inferior, and temporal areas). Images were taken only when the CP vector and the light beam vector were parallel. The OCT machine automatically drew a first line with a diameter of 3.45 mm in the superior and inferior directions and rotated a total of 12 radial lines clockwise. The RNFL thickness corresponding to the 12 radial lines was measured and represented as the average values of the quadrants.

The vertical and horizontal retina cross-sectional imaging were used to manually measure the length of the CP. The length of the CP was defined as the distance between the base of the CP immediately adjacent to the inner retina and the apex of the CP.

The retina map scan was used to evaluate retinal thickness by quadrant (superior, nasal, inferior, and temporal areas). When the desired retinal area

was taken, the retinal tomographic image was taken several times in the direction from superior to inferior. The software automatically measured the thickness of the retina using the horizontal cross-sectional images. The retina was divided into quadrants showing the mean value of total retinal thickness of each area quantitatively, and also the color classification according to the difference of thickness. Total retinal thickness was defined as the length from the internal limiting membrane (ILM) to the retinal pigment epithelium (RPE). The map was also divided into three circular regions (1 mm, 3 mm, and 5 mm in diameter) and centered at the CP. Taking into account the average size of a gecko eye identified in a previous study (Werner and Seifan, 2006), the parameters within the second circular region (3 mm in diameter) were selected to measure retinal thickness. If the CP was not in the center of the scan, we manually moved the zone to the correct position. Lastly, 3D images of the CP were obtained.

Using a quality-checking program installed in the software of the device, only good quality images were used for further data analysis. All measurements were made using the software included in the OCT instrument.

RESULTS

Physical and ophthalmic examination data from 8 geckos are shown in Table 1. A significant correlation was identified between the nose-cloaca distance and body weight (Spearman's correlation, $r = 0.896$, $P = 0.003$). Clear corneal surfaces, miotic pupils, and thick eyelids were identified using slit-lamp biomicroscope. In particular, multiple and vertical slit pupils were prominent when flashing a light (Fig. 1).

Table 1. Body length and body weight of Tokay geckos used in this study

Animal number	Nose-cloaca distance (cm)	Body weight (g)
1	13.0	35
2	13.5	37
3	14.0	44
4	15.0	58
5	12.0	30
6	14.5	51
7	14.0	40
8	14.0	35
Mean	13.8 ± 0.9	41.3 ± 9.0

Fig. 1. A photograph of the OS in case 4 magnified under a slit-lamp biomicroscope. The pupil shape was a vertical narrow slit with pseudopolychoria. The eyelid thickly covered the peripheral cornea.

1. Central corneal thickness and anterior chamber depth

On the OCT scan, the cornea was bright, thin, and curved. A hyperreflective line at the anterior corneal boundary and some lamellar layers inside the cornea were identified (Fig. 2). The boundaries between the spectacle, corneal epithelium and stroma were difficult to distinguish. The anterior chamber was imaged with a deep and dark area. The iris appeared as a brightest structure with irregular surface. The anterior lens capsule appeared as a thin and bright layer. The mean values of CCT and ACD were 177.6 ± 20.9 μm and 1205.0 ± 79.9 μm, respectively (Table 2). In the gecko eyes, a significant correlation was identified between the CCT and body weight ($r = 0.755$, $P = 0.001$), and nose-cloaca distance ($r = 0.602$, $P = 0.014$) when Spearman's rank order correlation was used for statistical analyses.

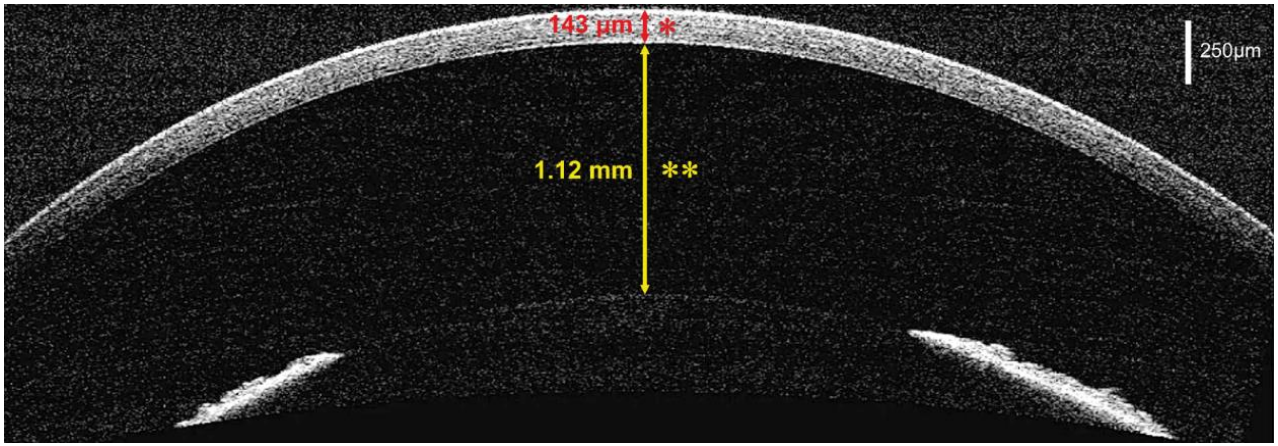

Fig. 2. The anterior segment of the OS in case 5 on OCT image. The thicknesses of the cornea (single red asterisk) and anterior chamber (double yellow asterisks) were measured manually.

Table 2. Cornea thickness and anterior chamber depth in gecko eyes

Scan type	Mean ± SD (µm)	Median ± SD (µm)	Minimum ± SD (µm)	Maximum ± SD (µm)
CCT	177.6 ± 20.9	181	143	219
ACD	1205.0 ± 79.9	1210	1100	1380

SD, standard deviation; CCT, central corneal thickness; ACD, anterior chamber depth.

2. Retinal nerve fiber layer thickness, conus papillaris length, and retinal thickness

In the ONH scan, if the edge of the CP boundary was not automatically recognized, the boundary marker was manually moved to the end of the RPE at the CP margin. The mean value of RNFL thickness of all four quadrants was 52.0 ± 8.2 μm. The mean values of RNFL thickness of superior, nasal, inferior, and temporal area were 61.3 ± 12.4 μm, 46.6 ± 7.8 μm, 51.1 ± 12.2 μm and 48.6 ± 10.0 μm, respectively. The RNFL thickness was the highest in the superior area, followed by the inferior, temporal, and nasal areas (Table 3).

In the retina cross-section scan, the mean value of CP length was 1546.4 ± 208.8 μm. The length of the CP was calculated in 14 eyes. Two of the sixteen eyes were excluded from the data because of poor-quality scans and the exact value could not be measured. The vitreal surface of the CP appeared to be a bright area, but inner aspect of the CP was seen as a dark area because the OCT light could not penetrate deep through the CP. The CP also blocked the light from going through the retinas so that some retinas were obscured by black shading (Fig. 3).

In the retina map scan, total retinal layers thickness was measured automatically (Fig. 4). The OCT unit recognized the border of the retinal layers and drawn retinal segment lines. If it was not recognized properly, the segment lines were corrected or the images were taken again to obtain

a good quality image. Reliable data were selected by comparing the manually measured values using the reference points of the segment lines. The total retinal layer thickness was the highest in the temporal area and the lowest in the inferior areas (Table 4). On the magnified tomographic retinal images, the nerve fiber layer (NFL) was shown as broad bright areas (Fig. 5). The ganglion cell layer (GCL) and the inner plexiform layer (IPL) were relatively darker than the NFL. However, there were certain areas where the three layers could not be distinguished. The inner nuclear layer (INL) and the outer nuclear layer (ONL) were shown as black stripes. The photoreceptor layer (PRL) was shown as a quite bright area.

In the 3D view, the CP and peripheral retinas were represented by 3D images (Fig. 6). If there was an area that the examiner wanted to see in detail in the 3D images, the area could be seen as tomographic images.

Table 3. Retinal nerve fiber layer thickness, conus papillaris length and retinal thickness in gecko eyes

Scan type	Mean ± SD (µm)	Median ± SD (µm)	Minimum ± SD (µm)	Maximum ± SD (µm)
ONH scan				
RNFL-average	52.0 ± 8.2	49.5	43	71
RNFL-superior	61.3 ± 12.4	64.5	41	78
RNFL-nasal	46.6 ± 7.8	47.0	34	61
RNFL-inferior	51.1 ± 12.2	50.5	33	74
RNFL-temporal	48.6 ± 10.0	47.5	36	76
Retina cross-section scan				
CP length[a]	1546.4 ± 208.8	1550.0	1220	1870
Total retinal thickness				
All quadrants	202.5 ± 9.4	203.6	190	219
Superior	204.8 ± 11.5	206.0	183	224
Nasal	202.8 ± 9.1	201.5	185	216
Inferior	194.6 ± 9.8	194.5	179	213
Temporal	207.9 ± 13.4	209.0	190	233

SD, standard deviation; ONH, optic nerve head; RNFL, retinal nerve fiber layer; CP, conus papillaris.

[a]Two eyes were not included in the data because their quality was not good enough to measure the length.

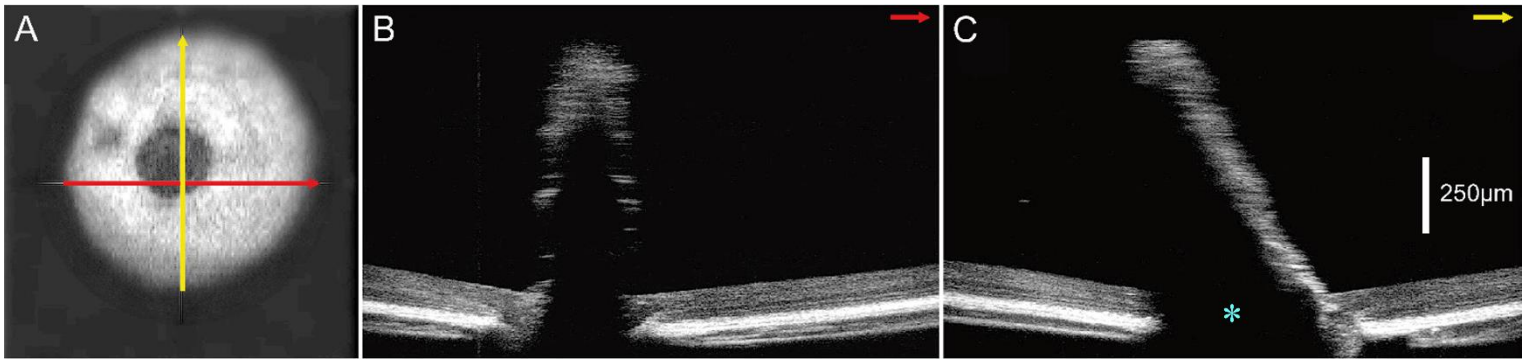

Fig. 3. An OCT image of the conus papillaris (CP) and retinal layers obtained from the OD in case 5. (A) In the en-face image, a guided view that provides a wide overview of retinal structures, the CP appears as a black area in the middle. The red and yellow arrows indicate the location of the horizontal and vertical section. The corresponding cross-sectional images are shown at B and C. (B) The horizontal section of the CP. Based on the CP, the left side shows the temporal area and the right side shows the nasal area of the retina. (C) The vertical section of the CP. Based on the CP, the left side shows the inferior area and the right side shows the superior area of the retina. Most CPs were slightly tilted to the inferior direction, which obscured some of retinas (*).

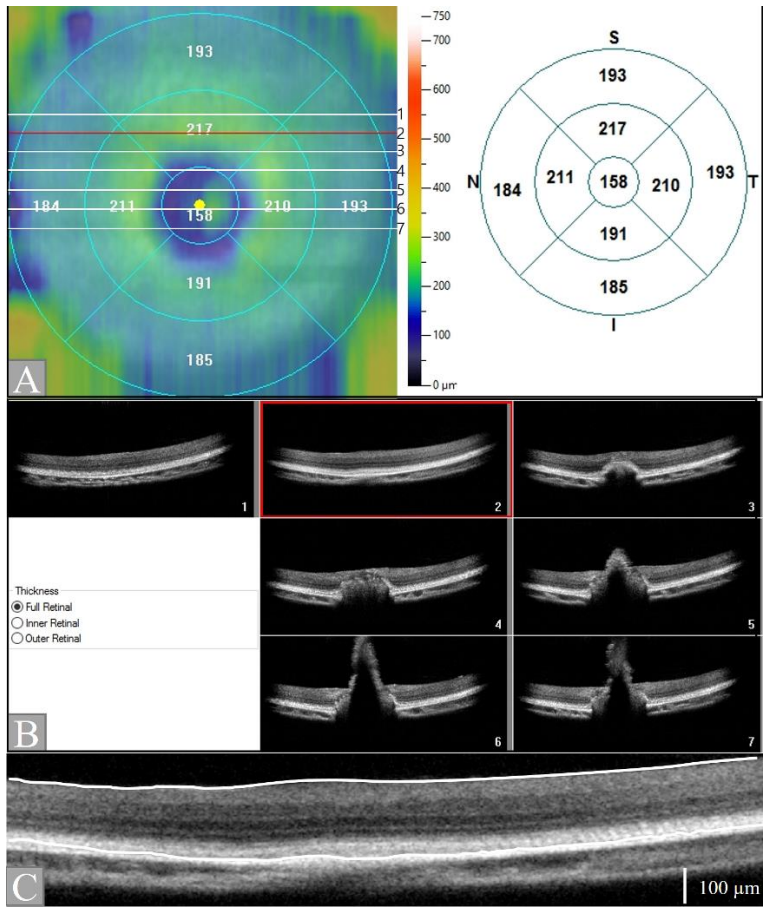

Fig. 4. Retina map obtained from the OS in case 2. (A) The image on the left shows the details of the retinal thickness in the circle using various colors corresponding to the difference of thickness of each area. Thicker areas are shown as red or yellow, and thinner areas as blue or green. The numbers and alphabet on the right image show the retinal thickness and position of the quadrants. Horizontal lines in the left circle image correspond to the OCT images taken in the horizontal cross section. Seven lines from the top to the bottom correspond to the images from number 1 to 7 in (B). (B) Tomographic images of the retina in the circle. There are several horizontal sections of the retina in the direction from superior to inferior.

The image inside the red square corresponds the cross section of the red horizontal line in (A). (C) Magnified cross-sectional image of the retina inside the red square in (B). The two thick white lines are the boundaries of the retina as recognized by the OCT device. Each line represents the inner limiting membrane and the outer boundary of the retinal pigment epithelium. S, superior; T, temporal; I, inferior; N, nasal

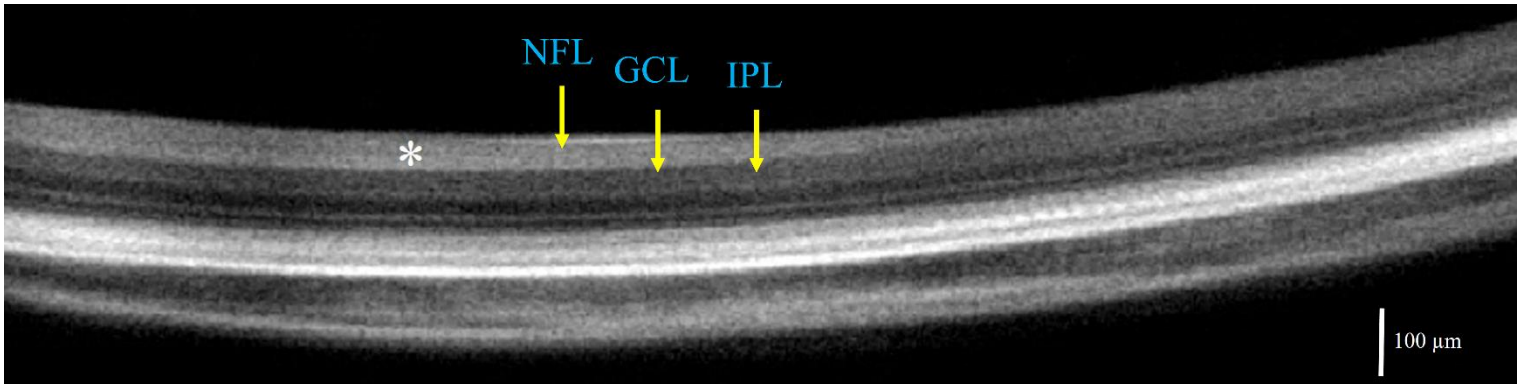

Fig. 5. Cross-section of gecko retina obtained from the OS in case 2. The image was taken from a region temporal to the conus papillaris (CP). The left side of the picture is the area near the CP, and the right side is far from the CP. The nerve fiber layer (NFL) is seen as bright areas (*) in the region near the CP. The NFL is indistinguishable from the ganglion cell layer (GCL) and the inner plexiform layer (IPL) in areas far from the CP.

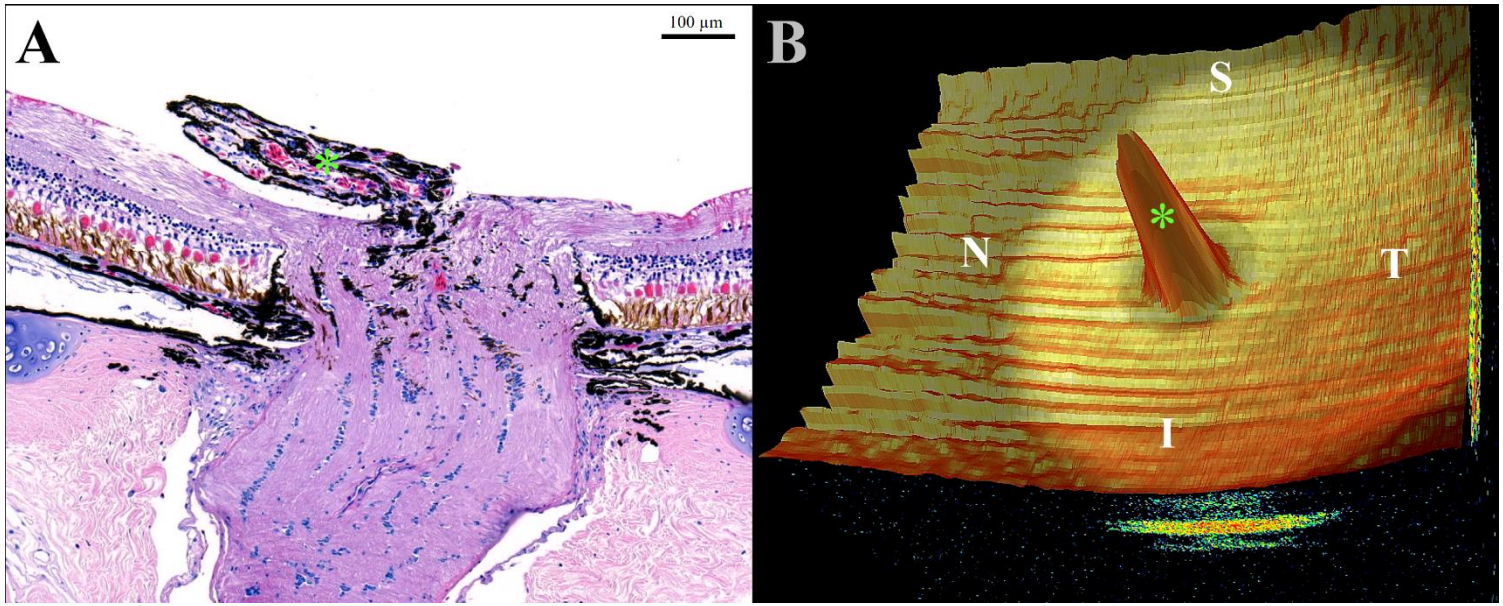

Fig. 6. Histological and three-dimensional OCT images of the conus papillaris (CP). (A) The CP (*) was observed as a structure originating from the optic nerve. (B) The CP (*) rises toward the vitreous body in the three-dimensional image. S, superior; T, temporal; I, inferior; N, nasal

3. Histological evaluation

A histological examination of one gecko retina was undertaken (Fig. 7). The NFL appeared thicker near the CP. The GCL consisted of mononuclear layer and the IPL was composed of a complex meshwork of fibrils. The INL consisted of four to seven nuclear layers, while the ONL consisted of mononuclear layer. The PRL was much thicker and more pronounced than other retinal layers.

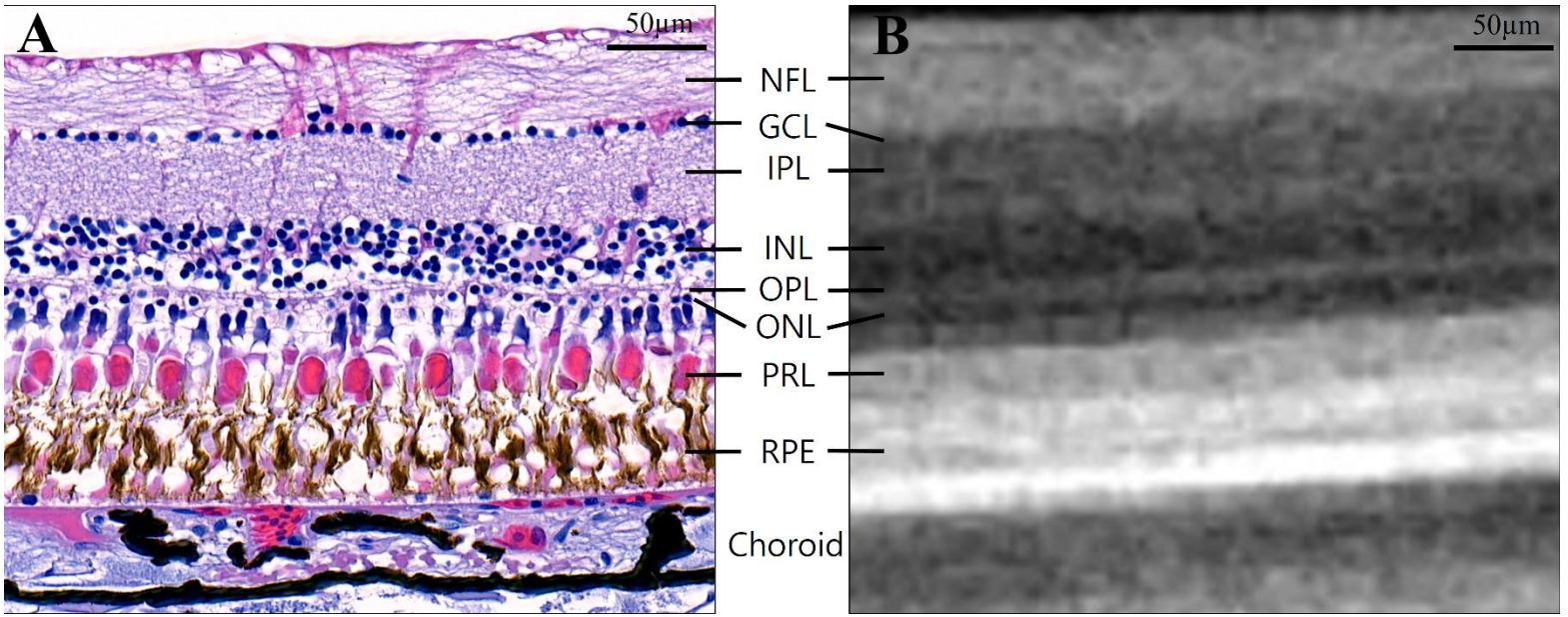

Fig. 7. Retinal layer segmentation of gecko retina by histology (A) and the corresponding OCT image (B). NFL, nerve fiber layer; GCL, ganglion cell layer; IPL, inner plexiform layer; INL, inner nuclear layer; OPL, outer plexiform layer; ONL, outer nuclear layer; PRL, photoreceptor layer; RPE, retinal pigment epithelium

DISCUSSION

The most geckos tend to have relatively large eyes for their body size (Werner, 1969). In addition, nocturnal geckos usually have larger eyes relative to their body size than diurnal geckos (Schmitz and Higham, 2018). Due to these characteristics, the Tokay gecko was selected as the experimental animal for OCT scanning in this study.

The mean value of CCT of the gecko in this study was 177.6 μm, which was higher than the 75 μm CCT of the nocturnal leopard gecko (Rival *et al*., 2015). The CCTs in other diurnal saurian species ranged from 50 to 200 μm (Rival *et al*., 2015). In the Tokay gecko species, there was a significant correlation between CCT and body weight, and nose-cloaca distance ($P < 0.05$). The SD-OCT unit used in this study calculated the CCT not as the thickness of a specific point, but as the mean thickness of a specific area (Graham *et al*., 2019; Wolfel *et al*., 2018). If the corneal thickness was thin below a certain standard, the machine did not automatically recognize the thickness. Therefore, some geckos with thin corneal thickness were not automatically measured. Eventually, the CCT was measured manually as the highest point of the cornea for consistency among animals. There were some difficulties in measuring the corneal thickness of the geckos. In general, the corneal epithelium appeared darker than the stroma. But gecko cornea was thinner than that of humans or dogs and the bright band of the air-to-cornea interface covered the anterior corneal epithelial boundary. As a result, no dark areas were identified in this study and it was difficult to distinguish the boundaries of the corneal epithelium and stroma. If OCT

imaging of lizards were performed during ecdysis, it could also have affected the measurement of the CCT. During spectacular ecdysis, the CCT could be measured as thicker than other normal lizards. A previous study described that spectacular ecdysis in the California king snake (*Lampropeltis getulus californiae*) increased the CCT baseline by up to 58.3% (Cazalot *et al*., 2015). In this study, there was no record of ecdysis in the geckos examined.

The thickness of the RNFL was the thickest in the superior area and the thinnest in the nasal area. There was a slight difference compared to a previous study in dogs showing that the superior area was the thickest and the inferior area the thinnest (Graham *et al*., 2019). The mean thickness of the RNFL of the Tokay gecko was 52.0 μm, which was about 25.7% of the 202.5 μm of the total retinal thickness. A previous study using light-electron micrographs showed that other nocturnal geckos' RNFL thickness ranged from 5 to 13 μm, and their total retinal thickness (not counting the RPE layer) ranged from 129 to 279 μm (Roll, 2001). The ratio of RNFL thickness to total retinal thickness differed considerably between this study and the previous study. In images of gecko retinas, the RNFL was indistinguishable from other layers (Fig. 5). This phenomenon was more prominent, especially as the distance from the CP increased. It was assumed that the measured value of RNFL thickness included the thickness of the ganglion cell layer (GCL) and some of IPL as well as RNFL, when the OCT unit calculated automatically. Also, because the thickness of the RNFL was taken around the CP, it could have been measured as thicker than it truly is. The RNFL was the thickest near the CP in histology (Fig. 6).

A previous study also showed that the RNFL thickness was the thickest near the optic nerve and the thinnest in the peripheral region of the retina (Roll, 2001).

Through OCT scanning, the images of living geckos' CPs were observed quite clearly. The anatomy of the Tokay gecko CP has long been known (Lüdicke, 1971). In the past, research on reptilian CPs was conducted mainly through the tissues of dead reptiles (Yovanovich *et al*., 2019; Brach, 1976; Zhao *et al*., 2019). Therefore, this study could be meaningful in that anatomical data of living geckos was obtained.

In the retina map scan, the mean value of total retinal thickness of all four quadrants was 202.5 μm. The Tokay gecko's retinal thickness was about medium compared to other nocturnal gecko's (Roll, 2001). However, the RNFL thickness was much thicker than other geckos. For Tokay gecko, the RNFL was expected to play a more important role than other nocturnal geckos, and could be a good experimental model for observing changes in RNFL thickness. In this study, the total retinal thickness was thickest in the temporal region and the thickness of the RNFL was thickest in the superior region. The optic nerve of many gecko species was observed to be slightly displaced inferionasally from the center of the retina in the previous histological study (Roll, 2001). The areas noted in the two studies showed the contrary areas, which means that the location of the optic nerve and the retinal thickness may influence each other.

The gecko retinal OCT image was compared with the gecko retinal histology in this study (Fig. 7). There was a close correspondence between the retinal layer segmentation in OCT imaging and segmentation in histology. Although the OCT

could not distinguish some thin retinal layers, such as the GCL, it was found that the overall thickness ratios of the various retinal layers to the total retinal thickness were similar to those in the histologic images.

Gecko eyeballs are very small and are an average of 8.3 mm in diameter (Werner and Seifan, 2006). Images of the peripheral retina could not have been easily obtained because the iris was not dilated completely. Accordingly, a diameter of 3 mm was selected instead of 5 mm in diameter. Unlike this study, the larger diameter zone was used to minimize the effect of the optic nerve and intraocular myelin on retinal thickness measurements of canine eyes in previous experiments (Graham *et al*., 2019).

The Tokay gecko is a nocturnal animal with a unique vertical slit pupil. Gecko irises are very light-sensitive and can change the size of the pupil more than 300-fold. It has been assumed to be a response to protect the pure rod retina against saturating light intensities (Denton, 1956). These features made geckos suitable for the study of pupil dynamics (Frankenberg, 1979). However, the feature was a disadvantage in this study. The pupils responded easily to low light, and severe pupil contraction disrupted observation and identification of retinal structure. Reptilian irises have striated sphincter muscles (Girling and Raiti, 2004), meaning that parasympathetic drugs commonly used in mammals are not effective in reptiles. Neuromuscular blockers, which are effective in birds with striated iris muscles, have not proven effective in reptiles (Ledbetter *et al*., 2017). Moreover, several reptile groups including geckos and all snakes have the spectacle as a layer of skin over the

cornea (Girling and Raiti, 2004). It forms an impermeable barrier to topical medications. Intra-cameral injection of medications for iris dilation was known to be only partially effective in mydriasis (Ledbetter *et al*., 2017). In this study, it was possible to take tomographic images of the retina by OCT after waiting for geckos to dilate the pupils themselves, but it was difficult to image the posterior segments of the eye with a fundus camera that needed a bright light source.

The first limitation was that the OCT machine was programmed for human or canine eyes. The eyeball size of the dog was about 20-22 mm (Gould and McLellan, 2014), which was more than twice the size of the gecko (8.3 mm) (Werner and Seifan, 2006). Even small movements by the geckos greatly influenced image analysis. The evaluations of ONH and RNFL are functions mainly applied to patients with glaucoma (Leung *et al*., 2010; Quigley *et al*., 1992; Guedes *et al*., 2003). In this experiment, however, it was simply used to measure the thickness of the RNFL around the CP. In addition, the original function of the retina map scan was to measure the thickness of the retina around the fovea in humans. The fovea locator function was included in the software to automatically identify and detect the fovea location within the OCT used in this study. However, nocturnal geckos do not have fovea or retinal vessels (Girling and Raiti, 2004; Roll, 2001). Therefore, the CP was used as a standard point, so this might affect measurements. The second limitation was that complete mydriasis has not been achieved. Further study on methods of pupil dilation in reptiles is needed for detailed retinal observations.

CONCLUSIONS

It was possible to take tomographic images of the anterior and posterior segments of the living gecko eye using an OCT unit. The thickness of the retina could be estimated, and the retinal layers were differentiated from layer to layer, although some layers were indistinct. Anatomical features of CP were also well-imaged. In the OCT scan, the thickness of the RNFL near the CP of Tokay geckos tended to be significantly thicker than other species. It was expected that the scientific and diagnostic application of OCT could be beneficial to other small exotic animals in addition to geckos.

REFERENCES

Bemis AM, Pirie CG, LoPinto AJ and Maranda L. Reproducibility and repeatability of optical coherence tomography imaging of the optic nerve head in normal beagle eyes. Veterinary Ophthalmology 2017; 20(6): 480-487.

Brach V. Structure and function of the ocular conus papillaris of *Anolis equestris* (Sauria: Iguanidae). Copeia 1976: 552-558.

Cazalot G, Rival F, Linsart A, Isard PF, Tissier M, Peiffer RL and Dulaurent T. Scanning laser ophthalmoscopy and optical coherence tomography imaging of spectacular ecdysis in the corn snake (*Pantherophis guttatus*) and the California king snake (*Lampropeltis getulus californiae*). Veterinary Ophthalmology 2015; 18: 8-14.

Denton EJ. The responses of the pupil of *Gekko gekko* to external light stimulus. Journal of General Physiology 1956; 40(2): 201-216.

Espinheira Gomes F, Parry S and Ledbetter E. Spectral domain optical coherence tomography evaluation of the feline optic nerve and peripapillary retina. Veterinary Ophthalmology 2019; 00: 1-10.

Fleishman LJ, Yeo AI and Perez CW. Visual acuity and signal color pattern in an Anolis lizard. Journal of Experimental Biology 2017; 220(12): 2154-2158.

Frankenberg E. Pupillary response to light in gekkonid lizards having various times of daily activity. Vision Research 1979; 19(3): 235-245.

Gekeler F, Gmeiner H, Volker M, Sachs H, Messias A, Eule C, Bartz-Schmidt KU, Zrenner E and Shinoda K. Assessment of the posterior segment of the cat

eye by optical coherence tomography (OCT). Veterinary Ophthalmology 2007; 10(3): 173-178.

Girling SJ and Raiti P. In: BSAVA manual of reptiles 2nd ed. British small animal veterinary association: Quedgeley, UK, 2004; 199-202.

Gould D and McLellan GJ. In: BSAVA manual of canine and feline ophthalmology 3rd ed. British Small Animal Veterinary Association: Quedgeley, UK, 2014; 28-29.

Graham KL, McCowan CI, Caruso K, Billson FM, Whittaker CJG and White A. Optical coherence tomography of the retina, nerve fiber layer, and optic nerve head in dogs with glaucoma. Veterinary Ophthalmology 2019; 00: 1-16.

Guedes V, Schuman JS, Hertzmark E, Wollstein G, Correnti A, Mancini R, Lederer D, Voskanian S, Velazquez L, Pakter HM, Pedut-Kloizman T, Fujimoto JG and Mattox C. Optical coherence tomography measurement of macular and nerve fiber layer thickness in normal and glaucomatous human eyes. Ophthalmology 2003; 110(1): 177-189.

Hernandez-Merino E, Kecova H, Jacobson SJ, Hamouche KN, Nzokwe RN and Grozdanic SD. Spectral domain optical coherence tomography (SD-OCT) assessment of the healthy female canine retina and optic nerve. Veterinary Ophthalmology 2011; 14(6): 400-405.

Higham TE and Schmitz L. A hierarchical view of gecko locomotion: photic environment, physiological optics, and locomotor performance. Integrative Comparative Biology 2019; 59: 443-455.

Ledbetter EC, de Matos R, Riedel RM and Southard TL. Phacoemulsification of bilateral mature cataracts in a Texas rat snake (*Elaphe obsoleta lindheimeri*). Journal of the American Veterinary Medical Association 2017; 251(11): 1318-1323.

Leung CK, Cheung CY, Weinreb RN, Qiu K, Liu S, Li H, Xu G, Fan N, Pang CP, Tse KK and Lam DS. Evaluation of retinal nerve fiber layer progression in glaucoma: a study on optical coherence tomography guided progression analysis. Investigative Ophthalmology & Visual Science 2010; 51(1): 217-222.

Lüdicke M. Ü ber die blutversorgung des auges von *Gekko gecko* (L.)(reptilia, sauria). Zeitschrift für Morphologie der Tiere 1971; 69(1): 23-47.

Osinchuk SC, Leis ML, Salpeter EM, Sandmeyer LS and Grahn BH. Evaluation of retinal morphology of canine sudden acquired retinal degeneration syndrome using optical coherence tomography and fluorescein angiography. Veterinary Ophthalmology 2019; 22(4): 398-406.

Putman BJ, Drury JP, Blumstein DT and Pauly GB. Fear no colors? Observer clothing color influences lizard escape behavior. PloS One 2017; 12(8): e0182146.

Quigley HA, Katz J, Derick RJ, Gilbert D and Sommer A. An evaluation of optic disc and nerve fiber layer examinations in monitoring progression of early glaucoma damage. Ophthalmology 1992; 99(1): 19-28.

Rival F, Linsart A, Isard PF, Besson C and Dulaurent T. Anterior segment morphology and morphometry in selected reptile species using optical coherence tomography. Veterinary Ophthalmology 2015; 18: 53-60.

Rodarte-Almeida AC, Petersen-Jones S, Langohr IM, Occelli L, Dornbusch PT, Shiokawa N and Montiani-Ferreira F. Retinal dysplasia in American pit bull terriers--phenotypic characterization and breeding study. Veterinary Ophthalmology 2016; 19(1): 11-21.

Roll B. Gecko vision-retinal organization, foveae and implications for binocular vision. Vision Research 2001; 41(16): 2043-2056.

Sannan NS, Shan X, Gregory-Evans K, Kusumi K and Gregory-Evans CY. *Anolis carolinensis* as a model to understand the molecular and cellular basis of foveal development. Experimental Eye Research 2018; 173: 138-147.

Schmitz L and Higham TE. Non-uniform evolutionary response of gecko eye size to changes in diel activity patterns. Biology Letters 2018; 14(5), 20180064.

Smith SD, Singh K, Lin SC, Chen PP, Chen TC, Francis BA and Jampel HD. Evaluation of the anterior chamber angle in glaucoma: a report by the american academy of ophthalmology. Ophthalmology 2013; 120(10): 1985-1997.

Somma AT, Moreno JCD, Sato MT, Rodrigues BD, Bacellar-Galdino M, Occelli LM, Petersen-Jones SM and Montiani-Ferreira F. Characterization of a novel form of progressive retinal atrophy in Whippet dogs: a clinical, electroretinographic, and breeding study. Veterinary Ophthalmology 2017; 20(5): 450-459.

Werner Y. Eye size in geckos of various ecological types (Reptilia: *Gekkonidae* and *Sphaerodactylidae*). Israel Journal of Ecology and Evolution 1969; 18(2-3): 291-316.

Werner YL and Seifan T. Eye size in geckos: Asymmetry, allometry, sexual dimorphism, and behavioral correlates. Journal of Morphology 2006; 267(12): 1486-1500.

Wolfel AE, Pederson SL, Cleymaet AM, Hess AM and Freeman KS. Canine central corneal thickness measurements via Pentacam-HR®, optical coherence tomography (Optovue iVue®), and high-resolution ultrasound biomicroscopy. Veterinary Ophthalmology 2018; 21(4): 362-370.

Wyneken J. Reptilian eyes and orbital structures. In: Proceedings 19th Annual Conference Association of Reptilian and Amphibian Veterinarians 2012; 75-82.

Yokoyama S and Blow NS. Molecular evolution of the cone visual pigments in the pure rod-retina of the nocturnal gecko, *Gekko gekko*. Gene 2001; 276(1-2): 117-125.

Yovanovich CA, Pierotti ME, Rodrigues MT and Grant T. A dune with a view: the eyes of a neotropical fossorial lizard. Frontiers in Zoology 2019; 16(1): 17.

Zhao Z, Goedhals J, Verdú-Ricoy J, Jordaan A and Heideman N. Comparative analysis of the eye anatomy in fossorial and surface-living skink species (Reptilia: Scincidae), with special reference to the structure of the retina. Acta Zoologica 2019; 00: 1-13.

국 문 초 록

광간섭 단층촬영을 이용한 게코 도마뱀 눈의 형태 측정

지도교수 서 강 문

고 석 민

서울대학교 대학원

수의학과 임상수의학 전공

본 연구는 스펙트럼 영역 광간섭 단층촬영(spectral-domain optical coherence tomography; SD-OCT)을 이용하여 게코 도마뱀 눈의 전방 및 후방 구조 이미지를 평가하고자 실시하였다.

안과 질환이 없는 8마리의 토케이 게코 도마뱀을 대상으로 실험을 진행하였다. 게코 도마뱀들의 코에서 총배설강까지의 길이 및 체중을 측정하였고, 마취제나 산동제 투여 없이 SD-OCT를 이용하여 안구의

단층 이미지를 얻었다. 기기 내 프로그램을 사용하여 수동적으로 중심각막 두께, 전안방의 깊이 및 유두상 원추체(conus papillaris)의 길이를 측정하였다. 유두상 원추체 주변의 망막신경 섬유층의 두께와 전체 망막층의 두께를 사분면으로 나누어 자동으로 측정하였다. 1마리의 게코 도마뱀을 안락사한 뒤 안구를 적출하여 망막의 조직학적 평가를 진행하였다.

코에서 총배설강까지의 평균 길이는 13.8 cm, 평균 체중은 41.3 g으로 측정되었다. 중심각막 평균 두께는 177.6 ㎛, 전안방의 평균 깊이는 1205.0 ㎛, 유두상 원추체의 평균 길이는 1546.4 ㎛로 측정되었다. 망막신경 섬유층의 평균 두께는 52.0 ㎛였으며, 사분면 중 상부 영역에서 가장 두꺼웠다. 전체 망막층의 평균 두께는 202.5 ㎛였으며, 측두 영역에서 가장 두꺼웠다. 게코 도마뱀 망막층들의 OCT 단층 영상과 조직학적 분할은 상당히 일치하였다.

본 연구에서 OCT를 이용하여 살아있는 게코 도마뱀 안구 구조를 단층 촬영할 수 있었다. 게코 도마뱀 망막 및 유두상 원추체의 해부학적 특징이 확인되었다. 포유류 외에도 조류, 파충류 등의 다른 동물들에게도 OCT의 연구, 진단적 적용이 가능할 것으로 기대한다.

주요어: 각막, 광간섭 단층촬영, 망막, 토케이 게코, 유두상 원추체

학번: 2018-26091